Maejo Int. J. Sci. Technol. **2016**, *10*(01), 25-40; doi: 10.14456/mijst.2016.3

Maejo International
Journal of Science and Technology

ISSN 1905-7873
Available online at www.mijst.mju.ac.th

Full Paper

Magnetohydrodynamic two-fluid flow and heat transfer in an inclined channel containing porous and fluid layers in a rotating system

Paramsetti Sri Ramachandra Murty [1, *] and Gudala Balaji Prakash [2]

[1] Department of Mathematics, Gitam University, Visakhapatnam, Pin code: 530 045, India
[2] Department of Mathematics, K. L. University, Guntur, Andhra Pradesh, Pin code: 522502, India
* Corresponding author, e-mail: drmurtypsr@gmail.com

Received: 20 June 2014/ Accepted: 23 December 2015 / Published: 21 January 2016

Abstract: Two-fluid convective flow between two infinitely long inclined parallel plates making an angle with the horizontal where the plates are maintained at different constant temperatures is studied. The upper phase is filled with a viscous fluid and also occupied by a porous material whereas the lower phase is filled with a different viscous fluid. It is assumed that both the fluids are incompressible with different viscosities, densities and thermal conductivities. The transport properties of the two fluids are taken to be constant. Further, the flow is assumed to be steady, laminar, fully developed and driven by a constant pressure gradient. The whole system is rotated with an angular velocity in a counter-clock-wise direction about an axis perpendicular to the plates. It is observed that the effect of increasing porous parameter is the decrease of temperature and primary and secondary velocities in both the phases.

Keywords: magnetohydrodynamics, two-fluid flow, heat transfer, rotating fluids, porous medium, inclined channel

---

INTRODUCTION

As the problems of fluid flow and heat transfer in porous media have enormous applications in science, engineering and technology, they have been studied by many researchers, notably Bian et al. [1], McWhirter et al. [2, 3], Geindreau and Auriault [4], Seddeek [5], Chauhan and Jain [6], Hayat et al. [7, 8] and Sunil and Mahajan [9]. More specifically, the existence of a fluid layer adjacent to a layer of fluid-saturated porous medium is a common occurrence in both geophysical and

Maejo Int. J. Sci. Technol. **2016**, *10*(01), 25-40; doi: 10.14456/mijst.2016.3

engineering environments. Convective flow and heat transfer between the fluid and porous layers had been studied by Prasad [10]. In 1998 Kuznetsov [11] studied Couette flow in a composite channel partially filled with a porous medium and partially with a clear fluid. Then in 2002 Krishna et al. [12] investigated hydromagnetic convection flow through a porous medium in a rotating channel. Effects of Hall current on magnetohydrodynamic flow in a rotating channel partially filled with a porous medium were analysed by Chauhan and Agrawal [13]. Recently, Chauhan and Rastogi [14, 15] considered Hall current and heat transfer effects on magnetohydrodynamic flow and magnetohydrodynamic Couette flow in a channel partially filled with a porous medium in a rotating system. Not much attention has been given to the flow and heat transfer in a fluid-superposed porous medium with inclined geometry except Malashetty and Umavathi [16] and Malashetty et al. [17, 18] even though the study is useful in many areas especially in geophysical systems. In this paper we undertake a study of hydromagnetic two-fluid flow with heat transfer aspects in an inclined channel containing a porous layer in the upper phase and a clear viscous fluid layer in the lower phase while the whole system is rotated about an axis perpendicular to the channel plates.

NOMENCLATURE

b	ratio of coefficients of thermal expansion, $\left(\frac{\beta_2}{\beta_1}\right)$
C_p	specific heat at constant pressure
Ec	Eckert number, $\left[\frac{(\bar{u}_1)^2}{C_p \Delta T}\right]$
g	acceleration due to gravity
h	ratio of heights of the two phases, $\left(\frac{h_2}{h_1}\right)$
Gr	Grashof number, $\left[\frac{g\,\beta_1 h_1^3 \Delta T}{\nu_1^2}\right]$
K	ratio of thermal conductivities, $\left(\frac{K_1}{K_2}\right)$
K_1, K_2	thermal conductivities of phase I and II respectively
k	permeability of porous medium
m	ratio of viscosities, $\left(\frac{\mu_1}{\mu_2}\right)$
n	ratio of densities $\left(\frac{\rho_2}{\rho_1}\right)$
P	non-dimensional pressure gradient, $\left[\frac{h_1^2\left(\frac{\partial p}{\partial x}\right)}{\mu_1 \bar{u}_1}\right]$
Pr	Prandtl number, $\left[\frac{\mu_1 C_p}{K_1}\right]$
Re	Reynolds number, $\left[\frac{\bar{u}_1 h_1}{\nu_1}\right]$

Maejo Int. J. Sci. Technol. **2016**, *10*(01), 25-40; doi: 10.14456/mijst.2016.3

R	rotation parameter, $\left[\frac{h_i(\sqrt{\Omega})}{\sqrt{\nu}}\right]$
T	temperature
$T_{w1}.T_{w2}$	temperature of boundaries
u	primary velocity
w	secondary velocity
$\bar{u}_1$	average velocity
$x.y,z$	space coordinates

Greek symbols

β	coefficient of thermal expansion
$\emptyset$	angle of inclination
ρ	density
ν	kinematic viscosity
μ	viscosity
λ	porous parameter
ε	product of Prandtl number and Eckert number $(Pr.Ec)$
ΔT	difference in temperature $[T_{w_1} - T_{w_2}]$
θ	non dimensional temperature, $\left[\frac{(T - T_{w2})}{\Delta T}\right]$
Ω	angular velocity

Subscript

i	value for phase

PROBLEM FORMULATION

The hydromagnetic two-phase convective flow between two infinitely long inclined parallel plates making an angle $\emptyset$ with the horizontal plane is considered, where the plates are maintained at different constant temperatures. The region $0 \leq y \leq h_1$ (Figure1) is filled with a viscous fluid and also occupied by a porous material having permeability k. The lower region $-h_2 \leq y \leq 0$ is filled with a different viscous fluid. It is assumed that both the fluids are incompressible with different viscosities μ_i, densities ρ_i and thermal conductivities K_i. Figure 1 represents the physical model of the problem.

Maejo Int. J. Sci. Technol. **2016**, *10*(01), 25-40; doi: 10.14456/mijst.2016.3

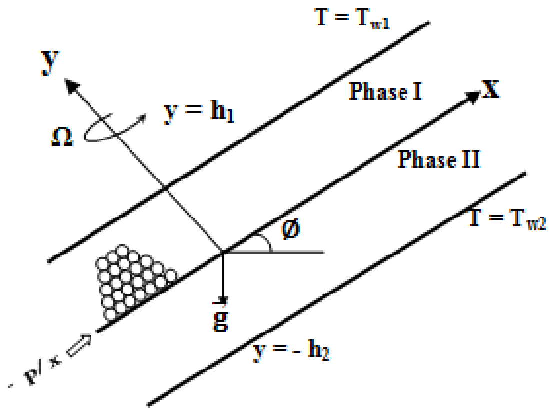

Figure 1. Physical model

The transport properties of the two fluids are taken to be constant. Further, the flow is assumed to be steady, laminar, fully developed and driven by a constant pressure gradient ($-\partial p/\partial x$). The whole system is rotated with an angular velocity Ω about the y-axis. The governing equations of motion and energy for phase I (porous medium) and phase II (clear viscous fluid) are formulated with the above assumptions.

In phase I we use the Darcy-Brinkman equations of motion for the flow through the porous medium so that no-slip conditions can be satisfied at the impermeable bounding wall for the porous layer and also for the compatibility conditions at the fluid – porous layer interface. The governing equations of motion and energy for Boussinesq fluid (following Malashetty et al. [18]) are:

$$\mu_1 \frac{d^2 u_1}{dy^2} + \rho_1 g \beta_1 \sin\phi (T_1 - T_{w2}) - \frac{\mu_1}{k} u_1 = \frac{\partial p}{\partial x} + 2\rho_1 \Omega w_1 , \tag{1}$$

$$\mu_1 \frac{d^2 w_1}{dy^2} - \frac{\mu_1}{k} w_1 = -2\rho_1 \Omega u_1 , \tag{2}$$

$$\frac{d^2 T_1}{dy^2} + \frac{\mu_1}{K_1}\left[\left(\frac{du_1}{dy}\right)^2 + \left(\frac{dw_1}{dy}\right)^2\right] + \frac{\mu_1}{K_1\, k}({u_1}^2 + {w_1}^2) = 0. \tag{3}$$

In phase II the governing equations of motion and energy for Boussinesq fluid (following Malashetty and Umavathi [16]) are:

$$\mu_2 \frac{d^2 u_2}{dy^2} + \rho_2 g \beta_2 \sin\phi \ (T_2 - T_{w2}) = \frac{\partial p}{\partial x} + 2\rho_2 \Omega w_2 , \tag{4}$$

$$\mu_2 \frac{d^2 w_2}{dy^2} = -2\rho_2 \Omega u_2 , \tag{5}$$

Maejo Int. J. Sci. Technol. **2016**, *10*(01), 25-40; doi: 10.14456/mijst.2016.3

$$\frac{d^2T_2}{dy^2}+\frac{\mu_2}{K_2}\left[\left(\frac{du_2}{dy}\right)^2+\left(\frac{dw_2}{dy}\right)^2\right]=0 \tag{6}$$

where u_i and w_i are the primary and secondary velocity components along x and z directions respectively, T_i is the temperature, β_i is the coefficient of thermal expansion and g is the acceleration due to gravity. The no-slip condition requires that the velocity must vanish at the walls. The suffixes 1 and 2 denote the values for phase I and phase II respectively. Following Beckermann et al. [19] and considering that the velocities, stresses, temperatures and heat fluxes are continuous across the fluid/porous medium with no slip of velocity, the boundary and interface conditions are:

$$u_1(h_1)=0,\ w_1(h_1)=0;\ u_1(0)=u_2(0),\ w_1(0)=w_2(0);\ u_2(-h_2)=0, w_2(-h_2)=0; \tag{7}$$

$$\mu_1\frac{du_1}{dy}=\mu_2\frac{du_2}{dy}\ \ and\ \ \mu_1\frac{dw_1}{dy}=\mu_2\frac{dw_2}{dy}\ \ at\ y=0. \tag{8}$$

Since the walls are maintained at constant different temperatures T_{w1} and T_{w2} at $y=h_1$ and $y=-h_2$ respectively, the boundary conditions on T_1 and T_2 are:

$$T_1(h_1)=T_{w1},\ \ T_1(0)=T_2(0),\ T_2(-h_2)=T_{w2},\ K_1\frac{dT_1}{dy}=K_2\frac{dT_2}{dy}\text{ at y=0.} \tag{9}$$

In making these equations dimensionless the following transformations are used:

$$u_1^*=\frac{u_1}{\bar{u}_1};\ \ u_2^*=\frac{u_2}{\bar{u}_1};\ \ y_1^*=\frac{y_1}{h_1};\ \ y_2^*=\frac{y_2}{h_2};\ \ \theta=\frac{(T-T_{w2})}{(T_{w1}-T_{w2})};\ \ m=\frac{\mu_1}{\mu_2};\ \ K=\frac{K_1}{K_2};$$

$$h=\frac{h_2}{h_1};\ \ n=\frac{\rho_2}{\rho_1};\ \ b=\frac{\beta_2}{\beta_1};\ \ Gr=\frac{g\,\beta_1\,h_1^3(T_{w1}-T_{w2})}{\nu_1^2};\ \ \lambda=\frac{h_1}{\sqrt{k}};\ \ \Pr=\frac{\mu_1\,C_p}{K_1};$$

$$P=\left(\frac{h_1^2}{\mu_1\bar{u}_1}\right)\left(\frac{\partial p}{\partial x}\right);\ \ \mathrm{Re}=\frac{\bar{u}_1\,h_1}{\nu_1};\ \ Ec=\frac{\bar{u}_1^2}{C_p(T_{w1}-T_{w2})};\ \ R^2=\frac{\Omega\,h_i^2}{\nu}.$$

With the above transformations, the governing equations (1-3) for phase I transform to:

$$\frac{d^2u_1}{dy^2}+\frac{Gr}{\mathrm{Re}}(\sin\phi)\theta_1-\lambda^2u_1=P+2R^2w_1\,, \tag{10}$$

$$\frac{d^2w_1}{dy^2}-\lambda^2w_1=-2R^2u_1\,, \tag{11}$$

$$\frac{d^2\theta_1}{dy^2}+\Pr Ec\left[\left(\frac{du_1}{dy}\right)^2+\left(\frac{dw_1}{dy}\right)^2\right]+\Pr Ec\,\lambda^2\,(u_1^2+w_1^2)=0\,. \tag{12}$$

Similarly, the governing equations (4-6) for phase II transform to:

Maejo Int. J. Sci. Technol. **2016**, *10*(01), 25-40; doi: 10.14456/mijst.2016.3

$$\frac{d^2u_2}{dy^2}+\frac{Gr}{\mathrm{Re}}b\ m\ n\ h^2(\sin\phi)\theta_2=mh^2P+2R^2w_2\,, \tag{13}$$

$$\frac{d^2w_2}{dy^2}=-2R^2u_2\,, \tag{14}$$

$$\frac{d^2\theta_2}{dy^2}+\mathrm{Pr}\,Ec\frac{k}{m}\left[\left(\frac{du_2}{dy}\right)^2+\left(\frac{dw_2}{dy}\right)^2\right]=0\,. \tag{15}$$

The non-dimensional forms of the boundary and interface conditions (7-9) convert to:

$$u_1(1)=0;\quad w_1(1)=0;\quad u_1(0)=u_2(0);\quad w_1(0)=w_2(0);\quad u_2(-1)=0;\quad w_2(-1)=0; \tag{16}$$

$$\frac{du_1}{dy}=\frac{1}{mh}\frac{du_2}{dy}\quad \text{and}\quad \frac{dw_1}{dy}=\frac{1}{mh}\frac{dw_2}{dy}\ \text{at } y=0, \tag{17}$$

$$\theta_1(1)=1,\quad \theta_1(0)=\theta_2(0),\quad \theta_2(-1)=0,\quad \frac{d\theta_1}{dy}=\frac{1}{K\,h}\frac{d\theta_2}{dy}\ \ at\ \ y=0\,. \tag{18}$$

The asterisks have been dropped for simplicity. Further, writing $q_1 = u_1 + i\,w_1$, equations (10-12) for phase I can be written in complex forms as:

$$\frac{d^2q_1}{dy^2}+\frac{Gr}{\mathrm{Re}}(\sin\phi)\theta_1-\lambda^2q_1=P-2i\,R^2q_1\,, \tag{19}$$

$$\frac{d^2\theta_1}{dy^2}+\mathrm{Pr}Ec\left[\frac{dq_1}{dy}\frac{d\bar{q}_1}{dy}\right]+\mathrm{Pr}Ec\lambda^2\left[q_1\,\bar{q}_1\right]=0. \tag{20}$$

Using $q_2 = u_2 + i\,w_2$, equations (13-15) for phase II can be written in complex forms as:

$$\frac{d^2q_2}{dy^2}+\frac{Gr}{\mathrm{Re}}b\ m\ n\ h^2(\sin\phi)\theta_2=mh^2P-2i\,R^2q_2\,, \tag{21}$$

$$\frac{d^2\theta_2}{dy^2}+\mathrm{Pr}\,Ec\frac{k}{m}\left[\frac{dq_2}{dy}\frac{d\bar{q}_2}{dy}\right]=0\,. \tag{22}$$

The corresponding boundary and interface conditions are:

$$q_1(1)=0\,,\quad q_1(0)=q_2(0)\,,\quad q_2(-1)=0\,,\quad \frac{dq_1}{dy}=\frac{1}{mh}\frac{dq_2}{dy}\ \ at\ \ y=0\,, \tag{23}$$

$$\theta_1(1)=1\,,\quad \theta_1(0)=\theta_2(0)\,,\quad \theta_2(-1)=0\,,\quad \frac{d\theta_1}{dy}=\frac{1}{K\,h}\frac{d\theta_2}{dy}\ \ at\ \ y=0\,. \tag{24}$$

Maejo Int. J. Sci. Technol. **2016**, *10*(01), 25-40; doi: 10.14456/mijst.2016.3

SOLUTIONS OF THE PROBLEM

The governing equations of motion (19), (21) and of energy (20), (22) are to be solved subject to the boundary and interface conditions (23) and (24). Due to the inclusion of the dissipation terms, the equations are coupled and non-linear, and their solutions are obtained using perturbation technique. Since the Eckert number is of order 10^{-5} and is very small, the product Pr Ec (=ε) is very small and is used in the regular perturbation method. The solutions are assumed in the following forms:

$$(q_1,\theta_1)=(q_{10},\theta_{10})+\varepsilon(q_{11},\theta_{11})+\ \ldots\ldots \tag{25}$$

$$(q_2,\theta_2)=(q_{20},\theta_{20})+\varepsilon(q_{21},\theta_{21})+\ldots\ \ldots \tag{26}$$

where q_{10}, q_{20} and θ_{10}, θ_{20} are solutions for the case ε equal to zero, and q_{11}, q_{21} and θ_{11}, θ_{21} are perturbed quantities related to q_{10}, q_{20} and θ_{10}, θ_{20} respectively. Substituting the above solutions in equations (19-22) and then equating the coefficients of similar powers of ε to zero, we get equations of zeroth-order and first-order approximations for phase I and phase II as follows.

Equations of zeroth-order approximation for phase I:

$$\frac{d^2q_{10}}{dy^2}+\frac{Gr}{\mathrm{Re}}(\sin\phi)\theta_{10}-\lambda^2 q_{10}=P-2i\,R^2 q_{10}\,, \tag{27}$$

$$\frac{d^2\theta_{10}}{dy^2}=0\,. \tag{28}$$

Equations of first-order approximation for phase I:

$$\frac{d^2q_{11}}{dy^2}+\frac{Gr}{\mathrm{Re}}(\sin\phi)\theta_{11}-\lambda^2 q_{11}=-2i\,R^2 q_{11}\,, \tag{29}$$

$$\frac{d^2\theta_{11}}{dy^2}+\left[\frac{dq_{10}}{dy}\,\frac{d\bar{q}_{10}}{dy}\right]+\lambda^2(q_{10}\,\bar{q}_{10})=0\,. \tag{30}$$

Equations of zeroth-order approximation for phase II:

$$\frac{d^2q_{20}}{dy^2}+\frac{Gr}{\mathrm{Re}}b\,m\,n\,h^2(\sin\phi)\ \theta_{20}=mh^2P-2i\,R^2 q_{20}\,, \tag{31}$$

$$\frac{d^2\theta_{20}}{dy^2}=0\,. \tag{32}$$

Equations of first-order approximation for phase II:

$$\frac{d^2q_{21}}{dy^2}+\frac{Gr}{\mathrm{Re}}b\,m\,n\,h^2(\sin\phi)\,\theta_{21}=-2i\,R^2 q_{21}\,, \tag{33}$$

$$\frac{d^2\theta_{21}}{dy^2}+\frac{k}{m}\left[\frac{dq_{20}}{dy}\,\frac{d\bar{q}_{20}}{dy}\right]=0\,. \tag{34}$$

The corresponding boundary conditions (23) and (24) transform to:

$$q_{10}(1)=0,\quad q_{10}(0)=q_{20}(0),\quad q_{20}(-1)=0,\quad \frac{dq_{10}}{dy}=\frac{1}{mh}\frac{dq_{20}}{dy}\ \ at\ \ y=0, \tag{35}$$

$$\theta_{10}(1)=1,\quad \theta_{10}(0)=\theta_{20}(0),\quad \theta_{20}(-1)=0,\quad \frac{d\theta_{10}}{dy}=\frac{1}{Kh}\frac{d\theta_{20}}{dy}\ \ at\ \ y=0, \tag{36}$$

$$q_{11}(1)=0,\quad q_{11}(0)=q_{21}(0),\quad q_{21}(-1)=0,\quad \frac{dq_{11}}{dy}=\frac{1}{mh}\frac{dq_{21}}{dy}\ \ at\ \ y=0, \tag{37}$$

$$\theta_{11}(1)=0,\quad \theta_{11}(0)=\theta_{21}(0),\quad \theta_{21}(-1)=0,\quad \frac{d\theta_{11}}{dy}=\frac{1}{Kh}\frac{d\theta_{21}}{dy}\ \ at\ \ y=0. \tag{38}$$

It is noted that $q_{10}=u_{10}+iw_{10}$, $q_{20}=u_{20}+iw_{20}$, $q_{11}=u_{11}+iw_{11}$ and $q_{21}=u_{21}+iw_{21}$.

Solutions of equations of zeroth-order approximation (27), (28) and (31), (32) using boundary conditions (35) and (36) are:

$$\theta_{10}=\frac{y+Kh}{1+Kh}, \tag{39}$$

$$\theta_{20}=\frac{Kh(1+y)}{1+Kh}, \tag{40}$$

$$u_{10}=\left[\left(c_{25}\,e^{m_5 y}+c_{26}\,e^{-m_5 y}\right)\cos(m_6 y)+(m_{14}+m_{12}y)\right], \tag{41}$$

$$w_{10}=-\left[\left(c_{25}\,e^{m_5 y}-c_{26}\,e^{-m_5 y}\right)\sin(m_6 y)-(m_{15}+m_{13}y)\right], \tag{42}$$

$$u_{20}=\left(c_{27}\,e^{Ry}+c_{28}\,e^{-Ry}\right)\cos(Ry), \tag{43}$$

$$w_{20}=\left(c_{28}\,e^{-Ry}-c_{27}\,e^{Ry}\right)\sin(Ry)+m_{18}+m_{19}y. \tag{44}$$

Solutions of equations of first-order approximation (29), (30) and (33), (34) using boundary conditions (37) and (38) are:

$$\begin{aligned}\theta_{11}=\{&c_{29}y+c_{30}-m_{127}\,e^{2m_5 y}+m_{128}\cos(2m_6 y)-m_{129}\,e^{-2m_5 y}-m_{189}\,e^{m_5 y}\cos(m_6 y)\\ &-m_{190}\,e^{m_5 y}\sin(m_6 y)-m_{191}\,e^{-m_5 y}\cos(m_6 y)-m_{192}\,e^{-m_5 y}\sin(m_6 y)\\ &-m_{193}\,e^{m_5 y}y\cos(m_6 y)-m_{194}\,e^{m_5 y}y\sin(m_6 y)-m_{195}\,e^{-m_5 y}y\cos(m_6 y)\\ &-m_{196}\,e^{-m_5 y}y\sin(m_6 y)-m_{161}y^4-m_{162}y^3-m_{163}y^2\}+i\,m_{164}\sin(2m_6 y)\\ &+i\{-m_{197}e^{m_5 y}\cos(m_6 y)-m_{198}\,e^{m_5 y}\sin(m_6 y)-m_{199}\,e^{-m_5 y}\cos(m_6 y)\}\\ &+i\{-m_{200}\,e^{-m_5 y}\sin(m_6 y)-m_{201}\,e^{m_5 y}y\cos(m_6 y)-m_{202}\,e^{m_5 y}y\sin(m_6 y)\}\\ &+i\{-m_{203}\,e^{-m_5 y}y\cos(m_6 y)-m_{204}\,e^{-m_5 y}y\sin(m_6 y)\},\end{aligned} \tag{45}$$

$$\theta_{21}=\{c_{31}y+c_{32}-m_{215}\,e^{2Ry}-m_{216}\cos(2Ry)-m_{217}\,e^{-2Ry}+m_{218}\,e^{-Ry}\sin(Ry)$$

Maejo Int. J. Sci. Technol. **2016**, *10*(01), 25-40; doi: 10.14456/mijst.2016.3

$$+m_{218}\,e^{-Ry}\cos(Ry)+m_{219}\,e^{Ry}\sin(Ry)-m_{219}\,e^{Ry}\cos(Ry)-m_{220}y^{2}\}$$
$$+i\{m_{222}\sin(2Ry)+m_{223}\,e^{Ry}\sin(Ry)+m_{223}\,e^{Ry}\cos(Ry)+m_{224}\,e^{-Ry}\sin(Ry)\}$$
$$+i\{-m_{224}\,e^{-Ry}\cos(Ry)\}, \quad (46)$$

$$u_{11}=(c_{33}\,e^{m_5 y}+c_{34}\,e^{-m_5 y})\cos(m_6 y)+n_{92}\,e^{2m_5 y}+n_{93}\,e^{-2m_5 y}+n_{94}\cos(2m_6 y)$$
$$-n_{95}\sin(2m_6 y)-n_{96}\,e^{m_5 y}y\sin(m_6 y)-n_{97}\,e^{m_5 y}y\cos(m_6 y)-n_{98}\,e^{-m_5 y}y\sin(m_6 y)$$
$$-n_{99}e^{-m_5 y}y\cos(m_6 y)-n_{100}e^{m_5 y}y^{2}\sin(m_6 y)-n_{101}e^{m_5 y}y^{2}\cos(m_6 y)$$
$$-n_{102}e^{-m_5 y}y^{2}\sin(m_6 y)-n_{103}\,e^{-m_5 y}y^{2}\cos(m_6 y)-n_{104}y^{4}-n_{105}y^{3}$$
$$-n_{106}y^{2}-n_{107}y-n_{108}, \quad (47)$$

$$w_{11}=(c_{34}\,e^{-m_5 y}-c_{33}\,e^{m_5 y})\sin(m_6 y)-n_{109}\,e^{2m_5 y}-n_{110}\,e^{-2m_5 y}+n_{111}\cos(2m_6 y)$$
$$+n_{112}\sin(2m_6 y)-n_{113}\,e^{m_5 y}y\sin(m_6 y)-n_{114}\,e^{m_5 y}y\cos(m_6 y)-n_{115}\,e^{-m_5 y}y\sin(m_6 y)$$
$$-n_{116}\,e^{-m_5 y}y\cos(m_6 y)-n_{117}\,e^{m_5 y}y^{2}\sin(m_6 y)-n_{118}\,e^{m_5 y}y^{2}\cos(m_6 y)$$
$$-n_{119}\,e^{-m_5 y}y^{2}\sin(m_6 y)-n_{120}\,e^{-m_5 y}y^{2}\cos(m_6 y)-n_{121}y^{4}-n_{122}y^{3}$$
$$-n_{123}y^{2}-n_{124}y-n_{125}, \quad (48)$$

$$u_{21}=c_{35}\,e^{Ry}\cos(Ry)+c_{36}\,e^{-Ry}\cos(Ry)+n_{142}\,e^{2Ry}+n_{143}\,e^{-2Ry}+n_{144}\cos(2Ry)$$
$$+n_{145}\sin(2Ry)-n_{146}\,e^{-Ry}y\cos(Ry)-n_{147}\,e^{Ry}y\cos(Ry)+n_{148}, \quad (49)$$

$$w_{21}=c_{36}\,e^{-Ry}\sin(Ry)-c_{35}\,e^{Ry}\sin(Ry)-n_{149}\,e^{2Ry}-n_{150}\,e^{-2Ry}+n_{151}\cos(2Ry)$$
$$-n_{152}\sin(2Ry)+n_{153}\,e^{Ry}y\sin(Ry)-n_{154}e^{-Ry}y\sin(Ry)-n_{155}y^{2}+n_{156}y+n_{157}. \quad (50)$$

The constants involved in equations (41-50) are not given for the sake of brevity. Solutions for equations of zeroth- and first-order approximations (27-34) are solved numerically by fixing some of the parameters, namely P = - 5, b = 1, Re = 5 and n = 1.5. The varying parameters are λ, Gr, ø , m, h, R and K. As the solutions of zeroth-order approximation are linear, only for first-order approximation the temperature profiles are drawn. This shows that the heat transfer up to zeroth -order approximation is due to the conduction only. In Figures 2-20, all the other parameters except the varying one are chosen from the set (λ, Gr, ø , m, h, R, K) = (2, 5, 30°, 0.5, 1, 1, 1).

RESULTS AND DISCUSSION

Magnetohydrodynamic two-fluid flow with heat transfer aspects between two infinitely long inclined parallel plates in a rotating system was studied analytically. The resulting differential equations were solved using perturbation method for obtaining approximate solutions for temperature and primary and secondary velocity distributions.

Maejo Int. J. Sci. Technol. **2016**, *10*(01), 25-40; doi: 10.14456/mijst.2016.3

Figures 2 and 3 represent the effect of porous parameter λ on primary and secondary velocities respectively. It can be observed that the effect of increasing porous parameter is the decrease in primary and secondary velocities in both the phases. This is because the drag caused by the porous matrix on the flow of the first phase also affects the flow of the free viscous fluid phase. It is also observed that the effect of large λ on the velocity field is more pronounced as compared to the small λ. Figures 4 and 5 show the effect of rotation parameter R on primary and secondary velocity distributions respectively. As the rotation parameter R increases, the primary velocity decreases because increasing rotation parameter increases the Coriolis force, which in turn opposes the buoyancy force. Hence the primary velocity is reduced. From Figure 5, it is noticed that as the rotation parameter R increases from (0.5, 1.5) and the secondary velocity w also increases, but outside this range as R increases, it decreases.

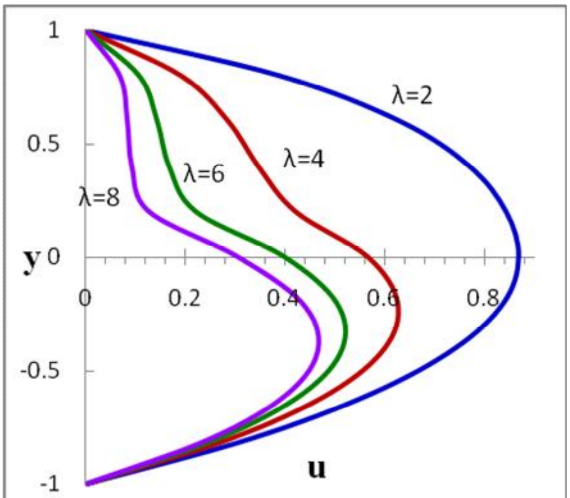

Figure 2. Primary velocity profiles for different values of porous parameter λ

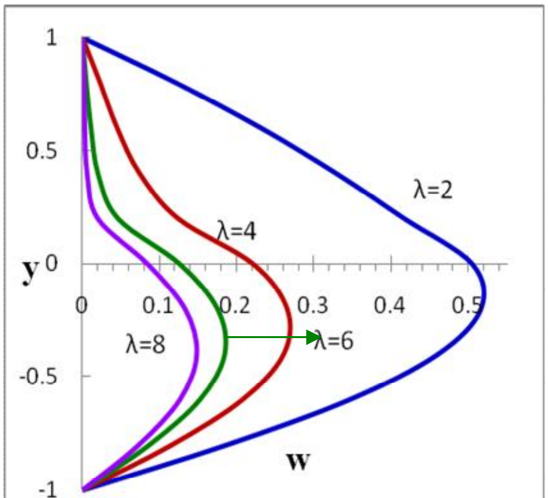

Figure 3. Secondary velocity profiles for different values of porous parameter λ

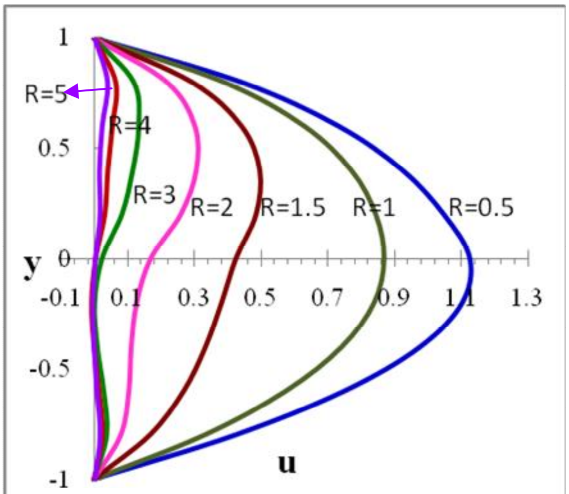

Figure 4. Primary velocity profiles for different values of rotation parameter R

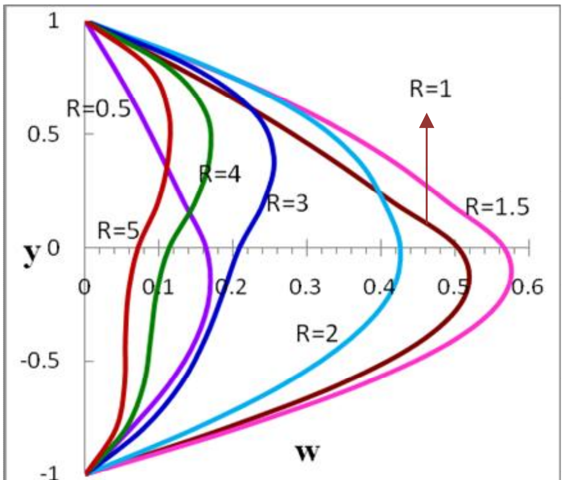

Figure 5. Secondary velocity profiles for different values of rotation parameter R

Maejo Int. J. Sci. Technol. **2016**, *10*(01), 25-40; doi: 10.14456/mijst.2016.3

The effect of Grashof number Gr on primary and secondary velocities is shown in Figures 6 and 7 respectively. As Grashof number increases both the velocities also increase because increasing Grashof number enhances the buoyancy force, which in turn supports the flow. The effect of inclination angle ø on primary and secondary velocities is represented in Figures 8 and 9. We observe that as the inclination angle ø increases, the primary and secondary velocities also increase in both phases. Figures 10 and 11 represent the effect of ratio of heights h on primary and secondary velocities respectively. It is noticed that increasing values of h increases both the velocities. This is because increasing the height of the clear viscous fluid increases both primary and secondary flows. The effect of ratio of viscosities m on primary and secondary velocities is shown in Figures 12 and 13. It is observed that both the velocities increase with increasing values of m.

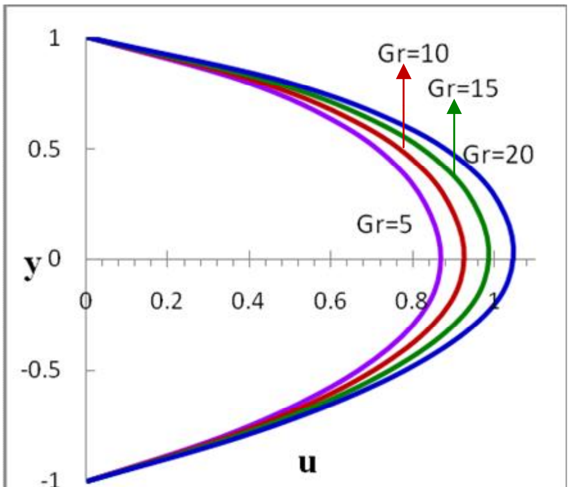

Figure 6. Primary velocity profiles for different values of Grashof number Gr

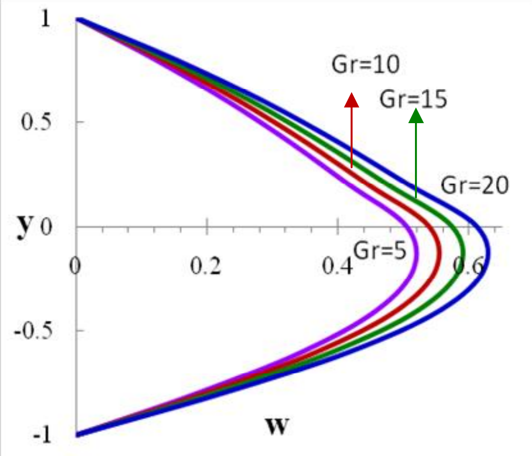

Figure 7. Secondary velocity profiles for different values of Grashof number Gr

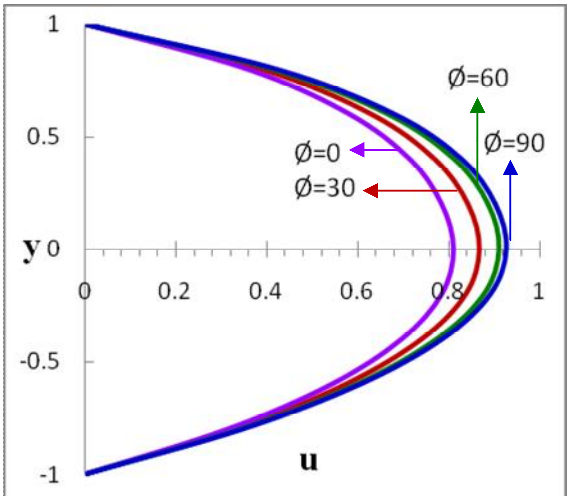

Figure 8. Primary velocity profiles for different values of angle of inclination Ø

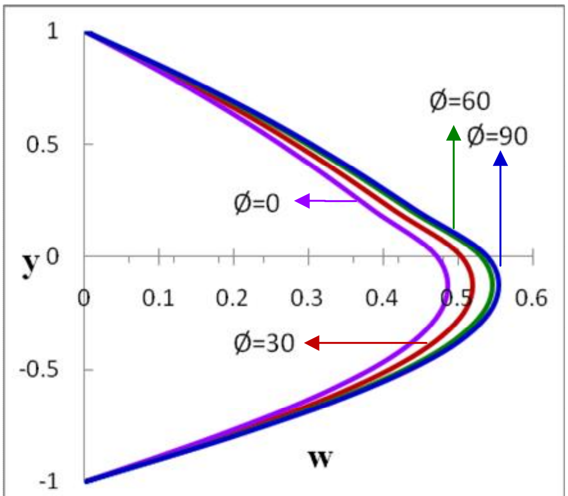

Figure 9. Secondary velocity profiles for different values of angle of inclination Ø

Maejo Int. J. Sci. Technol. **2016**, *10*(01), 25-40; doi: 10.14456/mijst.2016.3

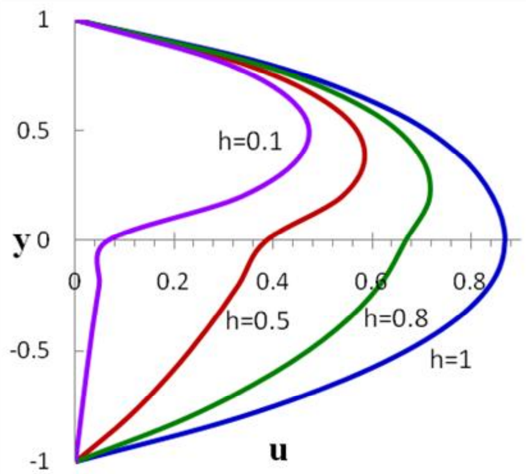

Figure 10. Primary velocity profiles for different values of ratio of heights h

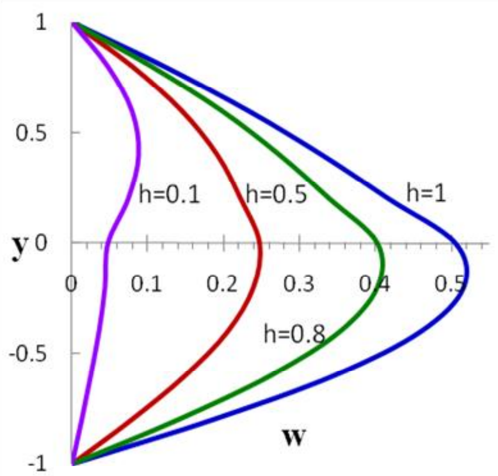

Figure 11. Secondary velocity profiles for different values of ratio of heights h

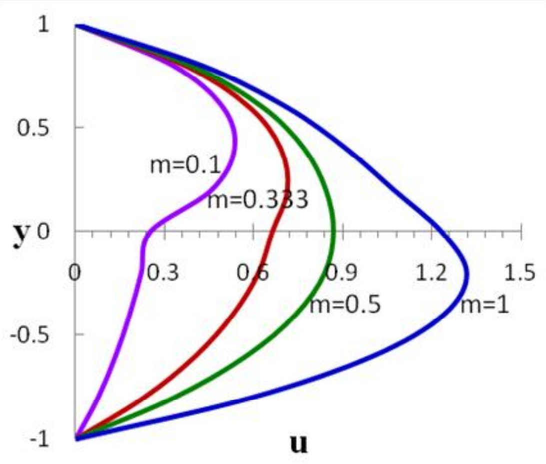

Figure 12. Primary velocity profiles for different values of ratio of viscosities m

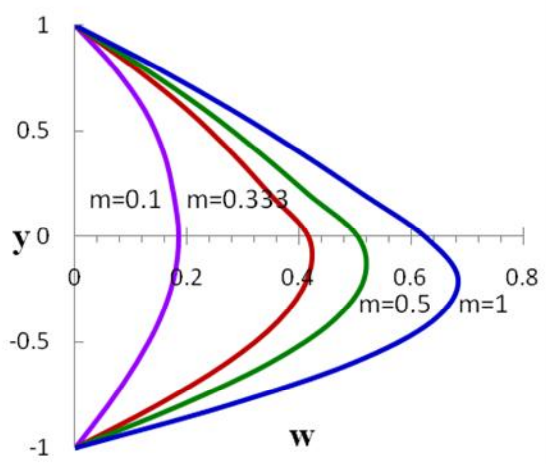

Figure 13. Secondary velocity profiles for different values of ratio of viscosities m

The effect of porous parameter λ on temperature distribution θ is shown in Figure 14. It is observed that, similar to its effect on the fluid flow, increasing the value of λ decreases the temperature field. Figure 15 represents the effect of rotation parameter R on temperature θ. As the rotation parameter R increases, the temperature decreases because increasing rotation increases the Coriolis force, which in turn opposes the buoyancy force. Thus, the velocity will be decreased, leading to a reduction in the temperature.

The effect of inclination angle ϕ on temperature is represented in Figure 16: as the inclination angle ϕ increases, the temperature also increases. Figure 17 exhibits the effect of the ratio of heights h on the temperature θ: increasing the value of h increases the temperature. The effect of Grashof number Gr on temperature θ is shown in Figure 18: an increase in Gr increases the temperature field in both phases. The effect of ratio of viscosities m of the two phases on temperature is the same as its effect on the velocities, as evident from Figure 19. Figure 20 shows the effect of the ratio of thermal

Maejo Int. J. Sci. Technol. **2016**, *10*(01), 25-40; doi: 10.14456/mijst.2016.3

conductivities K on temperature θ: the larger the ratio of thermal conductivities, the greater the amount of heat transfer.

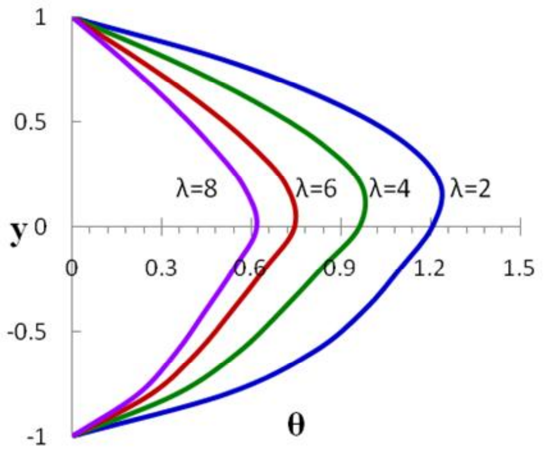

Figure 14. Temperature profiles for different values of porous parameter λ

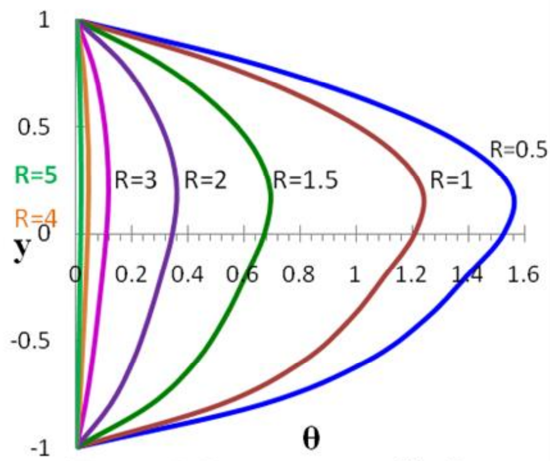

Figure 15. Temperature profiles for different values of rotation parameter R

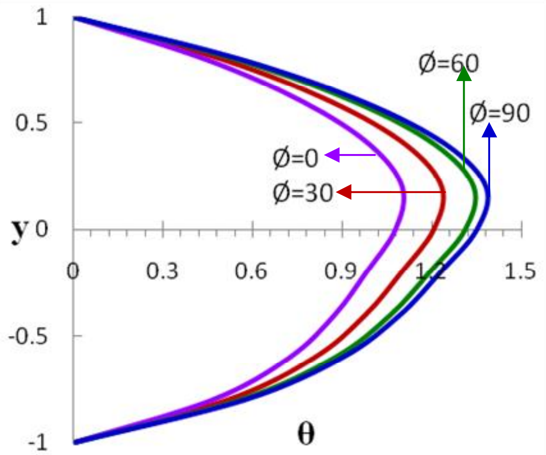

Figure 16. Temperature profiles for different values of angle of inclination Ø

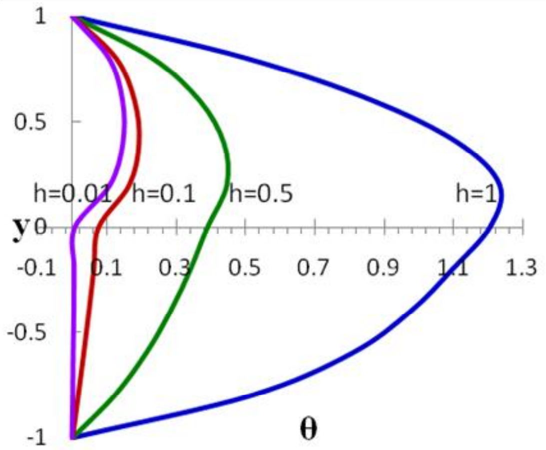

Figure 17. Temperature profiles for different values of ratio of heights h

Maejo Int. J. Sci. Technol. **2016**, *10*(01), 25-40; doi: 10.14456/mijst.2016.3

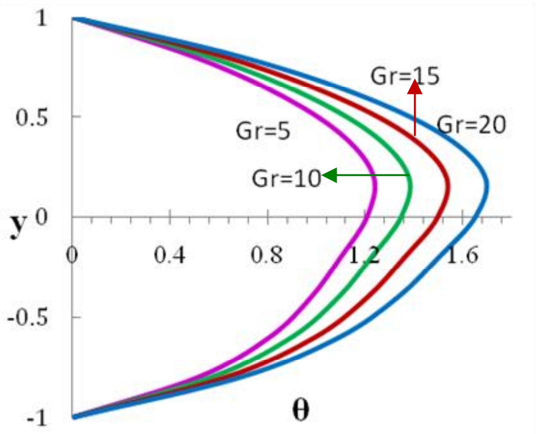

Figure 18. Temperature profiles for different values of Grashof number Gr

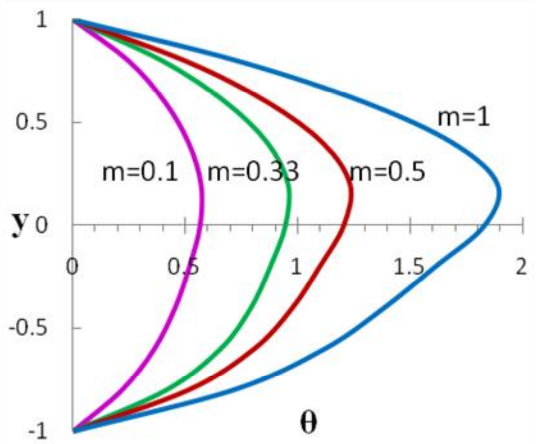

Figure 19. Temperature profiles for different values of ratio of viscosities m

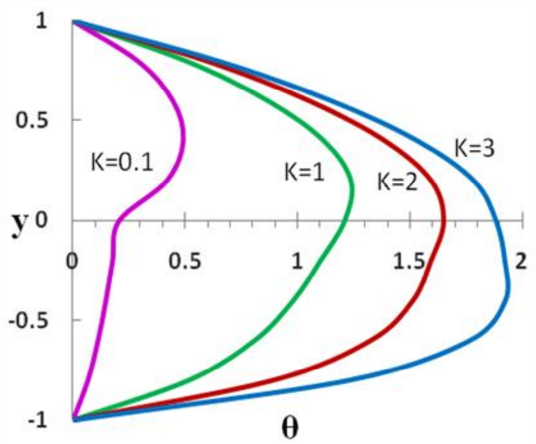

Figure 20. Temperature profiles for different values of ratio of thermal conductivities K

CONCLUSIONS

The problem of magnetohydrodynamic two-fluid convective flow and heat transfer in an inclined channel containing a viscous fluid superposed by the porous medium with constant permeability in a rotating system has been investigated analytically. Approximate solutions for temperature and primary and secondary velocities have been obtained using regular perturbation method. The important results from this study are:

- The effect of porous parameter is to retard the temperature and primary and secondary velocities in both phases.
- The increase in buoyancy force incorporated through Grashof number and angle of inclination is to enhance the temperature and primary and secondary velocities for both porous and viscous layers.

- The increase in Coriolis force incorporated through the rotation parameter is to reduce the temperature and primary velocity of the flow in both phases.
- The flow and thermal aspects of the fluids in the channel are enhanced by an increase in the ratio of viscosities of the fluids and the ratio of heights of the two phases.
- The results of the two-layered flow containing both the fluid and porous layers could be useful in recharge/discharge problems like the flow of geophysical fluids, packed-bed energy storage, etc.

REFERENCES

1. W. Bian, P. Vasseur, E. Bilgen and F. Meng, "Effect of an electromagnetic field on natural convection in an inclined porous layer", *Int. J. Heat Fluid Flow*, **1996**, *17*, 36-44.
2. J. D. McWhirter, M. E. Crawford, D. E. Klein and T. L. Sanders, "Model for inertialess magnetohydrodynamic flow in packed beds", *Fusion Sci. Technol*., **1998**, *33*, 22-30.
3. J. D. McWhirter, M. E. Crawford and D. E. Klein, "Magnetohydrodynamic flows in porous media II: Experimental results", *Fusion Sci. Technol*., **1998**, *34*, 187-197.
4. C. Geindreau and J. L. Auriault, "Magnetohydrodynamic flows in porous media", *J. Fluid. Mech*., **2002**, *466*, 343-363.
5. M. A. Seddeek, "Effects of magnetic field and variable viscosity on forced non-Darcy flow about a flat plate with variable wall temperature in porous media in the presence of suction and blowing", *J. Appl. Mech. Tech. Phys*., **2002**, *43*, 13-17.
6. D. S. Chauhan and R. Jain, "Three dimensional MHD steady flow of a viscous incompressible fluid over a highly porous layer", *Modell. Measure. Control B Mech. Therm.*, **2005**, *74*, 19-34.
7. T. Hayat, M. Husain and M. Khan, "Effects of Hall current on flows of a Burger's fluid through a porous medium", *Transp. Porous Med*., **2007**, *68*, 249-263.
8. T. Hayat, M. Javed and N. Ali, "MHD peristaltic transport of a Jeffery fluid in a channel with compliant walls and porous space", *Transp. Porous Med.*, **2008**, *74*, 259-274.
9. Sunil and A. Mahajan, "A nonlinear stability analysis for rotating magnetized ferrofluid heated from below saturating a porous medium", *Z. Angew. Math. Phys*., **2009**, *60*, 344-362.
10. V. Prasad, "Convective flow interaction and heat transfer between fluid and porous layers", in “Convective Heat and Mass Transfer in Porous Media, Part II” (Ed. S. Kakac, B. Kilkis, F. A. Kulacki and F. Arinc), Springer, Netherlands, **1991**, pp.563-615.
11. A. V. Kuznetsov, "Analytical investigation of Couette flow in a composite channel partially filled with a porous medium and partially with a clear fluid", *Int. J. Heat Mass Transf.*, **1998**, *41*, 2556-2560.
12. D. V. Krishna, D. R. V. Prasada Rao and A. S. R. Murthy, "Hydromagnetic convection flow through a porous medium in a rotating channel", *J. Eng. Phys. Thermophys.*, **2002**, *75*, 281-291.
13. D. S. Chauhan and R. Agrawal, "Effect of Hall current on MHD flow in a rotating channel partially filled with a porous medium", *Chem. Eng. Commun*., **2010**, *197*, 830-845.
14. D. S. Chauhan and P. Rastogi, "Hall current and heat transfer effects on MHD flow in a channel partially filled with a porous medium in a rotating system", *Turkish J. Eng. Environ. Sci*., **2009**, *33*, 167-184.

Maejo Int. J. Sci. Technol. **2016**, *10*(01), 25-40; doi: 10.14456/mijst.2016.3

15. D. S. Chauhan and P. Rastogi, "Heat transfer effects on rotating MHD Couette flow in a channel partially filled by a porous medium with Hall current", *J. Appl. Sci. Eng*., **2012**, *15*, 281-290.
16. M. S. Malashetty and J. C. Umavathi, "Two-phase magnetohydrodynamic flow and heat transfer in an inclined channel", *Int. J. Multiphase Flow*, **1997**, 23, 545-560.
17. M. S. Malashetty, J. C. Umavathi and J. P. Kumar, "Convective magnetohydrodynamic two fluid flow and heat transfer in an inclined channel", *Heat Mass Transf.*, **2001**, *37*, 259-264.
18. M. S. Malashetty, J. C. Umavathi and J. P. Kumar, "Convective flow and heat transfer in an inclined composite porous medium", *J. Porous Med.*, **2001**, *4*, 15-22.
19. C. Beckermann, R. Viskanta and S. Ramadhyani, "Natural convection in vertical enclosures containing simultaneously fluid and porous layers", *J. Fluid Mech.*, **1988**, *186*, 257-284.